

FUSE DETECTION OF DIFFUSE GALACTIC O VI EMISSION TOWARD THE COMA AND VIRGO CLUSTERS¹

W. VAN DYKE DIXON², SHAUNA SALLMEN, AND MARK HURWITZ
Space Sciences Laboratory, University of California, Berkeley, Berkeley, CA 94720-7450;
vand@ssl.berkeley.edu, sallmen@ssl.berkeley.edu, markh@ssl.berkeley.edu

AND

RICHARD LIEU
Department of Physics, University of Alabama in Huntsville, Huntsville, AL 35899; lieu@cspar.uah.edu
To appear in the Astrophysical Journal, Letters

ABSTRACT

We report the detection of diffuse O VI $\lambda\lambda 1032, 1038$ emission in a 29-ksec observation centered on the Coma Cluster ($l = 57.6, b = +88.0$) and an 11-ksec observation toward Virgo ($l = 284.2, b = +74.5$) through the $30'' \times 30''$ aperture of the *Far Ultraviolet Spectroscopic Explorer (FUSE)*. The emission lines have a redshift near zero and are thus produced by gas in our own Galaxy. Observed surface brightnesses are 2000 ± 600 photons $\text{cm}^{-2} \text{s}^{-1} \text{sr}^{-1}$ for each of the O VI components in the Coma spectrum, and 2900 ± 700 and 1700 ± 700 photons $\text{cm}^{-2} \text{s}^{-1} \text{sr}^{-1}$ for the 1032 and 1038 Å lines, respectively, toward Virgo. These features are similar in strength to those recently observed in the southern Galactic hemisphere ($l = 315.0, b = -41.3$) in an ~ 200 ksec *FUSE* observation. From a *FUSE* spectrum of M87, we find that $N(\text{O VI})$ toward Virgo is $(1.4 \pm 0.8) \times 10^{14} \text{cm}^{-2}$. By combining emission- and absorption-line data for this sight line, we estimate the physical parameters of the emitting gas.

Subject headings: Galaxy: general — ISM: general — ultraviolet: ISM

1. INTRODUCTION

Emission spectroscopy at extreme- and far-ultraviolet wavelengths will provide the key to our eventual understanding of the origin, distribution, and physical processes of the hot interstellar medium (ISM). Observing diffuse interstellar emission at these wavelengths has, however, proven technically challenging, and only a handful of detections have been obtained to date (Martin & Bowyer 1990; Dixon, Davidsen, & Ferguson 1996). Thus, the recent observation of diffuse Galactic O VI emission with the *Far Ultraviolet Spectroscopic Explorer (FUSE)* by Shelton et al. (2001) is both exciting, because of what it can tell us about the state and distribution of hot gas in the Galaxy, and frustrating, because of the long integration times (~ 200 ksec) required. We are therefore pleased to report the serendipitous detection of diffuse Galactic O VI emission in two (relatively) short *FUSE* observations of the Coma and Virgo Clusters. Combining our emission-line intensities toward Virgo with the O VI column density measured toward M87, we constrain the physical properties of the emitting gas. These results bode well for future efforts to map the sky at far-UV (FUV) wavelengths.

2. OBSERVATIONS AND DATA REDUCTION

FUSE comprises four separate optical systems. Two employ LiF optical coatings and are sensitive to wavelengths from 990 to 1187 Å, while the other two use SiC coatings, which provide reflectivity to wavelengths as short as 905 Å. The four channels overlap between 990 and 1070 Å. For a complete description of *FUSE*, see Moos et al. (2000) and Sahnou et al. (2000).

The *FUSE* spectrum of the Coma Cluster was obtained in 17 separate exposures on 2000 June 18 and 19. Each exposure was centered on $12^{\text{h}}59^{\text{m}}49^{\text{s}}.0, +27^{\circ}57'46''$ (J2000, or $l = 57.61, b = +87.96$ in Galactic coordinates), near the center of the Coma Cluster. The total exposure time was 28608 s, with 23553 s obtained during orbital night. We use the entire 29-ksec data set in our analysis. Our spectrum of the Virgo Cluster is a combination of data from two locations near the cluster center. Two exposures, centered on $12^{\text{h}}31^{\text{m}}07^{\text{s}}.3, +12^{\circ}23'46''$ ($l = 284.03, b = +74.52$) and totaling 2242 s, were obtained on 2000 June 13. Seven exposures, centered on $12^{\text{h}}31^{\text{m}}13^{\text{s}}.4, +12^{\circ}22'10''$ ($l = 284.15, b = +74.50$) and totaling 8688 s, were obtained on 2000 June 17. The total integration time is 10,930 s, all of it during orbital night. All observations were made through the $30'' \times 30''$ low-resolution (LWRS) aperture. The data-reduction procedures applied to these data are discussed in detail in Dixon et al. (2001) and are not repeated here.

While the resolution of the *FUSE* spectrograph is approximately 15km s^{-1} for a point source, diffuse emission filling the LWRS aperture yields a line profile that is well approximated by a top-hat function with a width of $\sim 106 \text{km s}^{-1}$. Our spectra are quite faint, so we bin the Coma data by 8 detector pixels, or about 15.5km s^{-1} . Approximately 7 of these bins are required to span a diffuse emission feature, providing ample sensitivity to its line profile. We bin the data from the shorter Virgo observation by 16 pixels. We distinguish between detector pixels and 8- or 16-pixel bins throughout this Letter. Because of the wide disparity in the effective areas of the various detector

¹ Based on observations made with the NASA-CNES-CSA *Far Ultraviolet Spectroscopic Explorer*. *FUSE* is operated for NASA by the Johns Hopkins University under NASA contract NAS5-32985.

² Current address: Department of Physics and Astronomy, The Johns Hopkins University, Baltimore, MD 21218

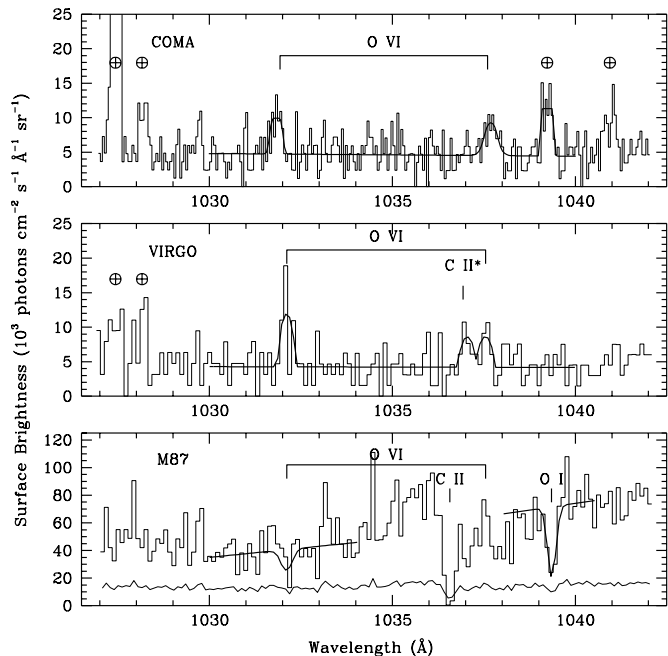


FIG. 1.— *FUSE* spectra of the (top) Coma and (middle) Virgo Clusters showing diffuse Galactic O VI $\lambda\lambda 1032, 1038$ emission. The Virgo spectrum also shows Galactic C II* $\lambda 1037.02$ emission. Terrestrial airglow features are marked with \oplus . The Coma spectrum is binned by 8 detector pixels, the Virgo spectrum by 16. The data, from detector LiF 1A, are presented as histograms and are overplotted by our best-fit models. The observed continuum level is consistent with the dark-count rate determined from unilluminated regions of the detector. The round shape of the model emission features in the Virgo spectrum (which are in fact top-hat functions) is an artifact of our sparse sampling of the model lines. Bottom: *FUSE* spectrum of M87, a weighted mean of the LiF 1A and LiF 2B spectra, binned by 16 detector pixels. The error spectrum is overplotted. Heavy lines are the best-fit O VI absorption model, with $N(\text{O VI}) = 1.4 \times 10^{14} \text{ cm}^{-2}$, and a Gaussian fit to the O I $\lambda 1039.23$ line, which we adopt as the absorption profile for O VI.

segments (Sahnou et al. 2000), combining faint spectra from different segments does not significantly improve their signal-to-noise ratio. We thus use data only from the segment with the highest effective area at the wavelength of interest.

The *FUSE* flux calibration, based on theoretical models of white-dwarf stellar atmospheres, is believed accurate to about 10% (Sahnou et al. 2000). Corrections to the nominal *FUSE* wavelength scale are derived from the measured positions of airglow features in the day-time Coma spectrum and are good to about 0.01 Å. Error bars are assigned to the data assuming Gaussian statistics, then smoothed by 9 bins to remove small-scale features in the error spectrum without significantly changing its shape. Segments of the flux- and wavelength-calibrated LiF 1A spectra of each cluster, showing the region about O VI $\lambda\lambda 1032, 1038$, are presented in Fig. 1. Upper limits on the redshifted emission from both clusters are presented in Dixon et al. (2001).

3. SPECTRAL ANALYSIS

In our analysis, model spectra are fit to the flux-calibrated data using the nonlinear curve-fitting program

TABLE 1
O VI EMISSION FEATURES

Wavelength (Å)	Surface Brightness ($\text{ph cm}^{-2} \text{s}^{-1} \text{sr}^{-1}$)	Intrinsic FWHM (km s^{-1})	LSR Velocity (km s^{-1})
Coma			
1031.83 ± 0.03	2000 ± 600	23 ± 55	-17 ± 9
1037.70 ± 0.06	2000 ± 600	75 ± 60	$+35 \pm 17$
Virgo			
1032.11 ± 0.05	2900 ± 700	< 80	$+84 \pm 15$
1037.55 ± 0.06	1700 ± 700	< 110	$+12 \pm 17$

NOTE.— Error bars are statistical and represent a change in χ^2 of 1.0. Uncertainties in the area of the LWRs aperture and the *FUSE* flux calibration contribute an additional 14% systematic uncertainty to the quoted line fluxes. For lines narrower than our top-hat function, 1- σ upper limits to the intrinsic FWHM are quoted.

SPECFIT (Kris 1994), which runs in the IRAF³ environment, to perform a χ^2 minimization of the model parameters. The observed profile of a diffuse emission feature represents a convolution of its intrinsic profile, assumed to be a Gaussian, with the 106 km s^{-1} top-hat function discussed above. Free parameters in the fit are the level and slope of the continuum (assumed linear) and the intensity, wavelength, and intrinsic FWHM of each emission line. The observed continuum level is consistent with the dark-count rate determined from unilluminated regions of the detector (Dixon et al. 2001).

The model that best fits our Coma spectrum between 1030 and 1040 Å yields a χ^2 of 166.7 for 173 degrees of freedom, including the O I $\lambda 1039.23$ airglow line. The Virgo spectrum, taken at night, does not show the O I feature, but does show emission from C II* $\lambda 1037.02$. (Significant C II $\lambda 1036.34$ emission is not expected; Shelton et al. 2001). The best-fit model returns a χ^2 of 80.4 for 85 degrees of freedom. These models are overplotted on the data in Fig. 1. Parameters of the best-fit O VI lines are presented in Table 1, those of the C II* line in Table 2. In both tables, error bars for each model parameter are determined by increasing the best-fit value of that parameter, while re-optimizing the other model parameters, until χ^2 increases by 1.0 (corresponding to a 1- σ deviation for one interesting parameter; Avni 1976). Because our wavelength scale is based on the measured positions of airglow lines, derived velocities are geocentric, and conversion to the Local Standard of Rest (LSR; Mihalas & Binney 1981) is straightforward.

We use the arguments of Shelton et al. (2001) to reject four alternative explanations for the emission observed in the 1030–1040 Å region of the LiF 1A spectrum: scattered light in the cross-dispersion direction on the detector, atmospheric airglow emission, solar O VI contamination, and H₂ fluorescence. Furthermore, none of the observed features can be identified as redshifted emission from either background cluster. We conclude that the observed features represent diffuse Galactic emission.

To search for statistically-significant emission at other wavelengths, we bin each spectrum to the instrument resolution and identify individual resolution elements with a signal-to-noise ratio greater than 3. Each such peak corresponds to a single emission feature. Returning to our nominally-binned spectrum, we fit each feature with

³ The Image Reduction and Analysis Facility (IRAF) is distributed by the National Optical Astronomy Observatories, which is operated by the Association of Universities for Research in Astronomy, Inc., (AURA) under cooperative agreement with the National Science Foundation.

TABLE 2
ADDITIONAL SPECTRAL FEATURES

Wavelength (Å)	Surface Brightness (ph cm ⁻² s ⁻¹ sr ⁻¹)	Intrinsic FWHM (km s ⁻¹)	Detector Segment	Identification
Coma				
977.04 ± 0.08	3500 ± 2400	43 ± 140	SiC 2A	C III λ977.020
1014.92 ± 0.09	2600 ± 700	120 ± 50	LiF 1A	S III λ1015.505
1122.17 ± 0.04	1600 ± 500	< 40	LiF 2A	C I λ1122.260
1138.96 ± 0.02	1800 ± 500	< 15	LiF 2A	Artifact?
1144.94 ± 0.06	2000 ± 600	< 50	LiF 2A	Fe II λ1144.938
Virgo				
975.17 ± 0.04	6400 ± 1500	< 40	SiC 2A	...
977.15 ± 0.12	7700 ± 3300	117 ± 130	SiC 2A	C III λ977.020
1037.04 ± 0.07	1700 ± 700	< 110	LiF 1A	C II* λ1037.018

NOTE.— See note to Table 1. To minimize contamination by solar emission, upper limits for the SiC 2A channel are derived only from data obtained during orbital night.

a linear continuum and model emission line. Because our data are rather noisy, we employ two measures of a feature's statistical significance. First, we determine the 1- σ uncertainty in its measured flux using the $\Delta\chi^2 = 1$ test described above; second, we test whether deleting the feature from our best-fit model raises χ^2 by at least 9 (corresponding to a 3- σ deviation for one interesting parameter, in this case the flux in the line; Avni 1976). We list in Table 2 those features that are significant at the 3- σ level by both tests, with three exceptions: First, we discard any features detected in known stray-light stripes (see Dixon et al. 2001). Second, we include the C II* λ1037 line in the Virgo spectrum to facilitate comparison with a similar feature seen by Shelton et al. (2001). Third, we include the C III λ977 feature, not seen by Shelton et al., because it is present in both of our spectra.

Two lines presented in Table 2 remain unidentified. Because it is so narrow, we suggest that the λ1138.96 feature in the Coma spectrum may represent a statistical fluctuation or detector artifact. The λ975.17 feature in the Virgo spectrum might be redshifted Ly γ , but its wavelength is too short: the line would appear at 976.04 Å at the redshift of Virgo ($z = 0.0036$; Ebeling et al. 1998) and 976.78 Å at that of M87 ($z = 0.00436$; Smith et al. 2000). Furthermore, most excitation mechanisms would produce more Ly β than Ly γ emission, and redshifted Ly β is not seen in this spectrum (Dixon et al. 2001).

4. N(O VI) TOWARDS M87

Given the emission intensity and column density of an emitting species along a given line of sight, one can derive the electron density and thermal pressure of the emitting plasma (Shull & Slavin 1994). We have the O VI intensity toward Virgo; to constrain its column density, we consider a *FUSE* spectrum of M87, the central galaxy of the Virgo Cluster.

Two night-time exposures, totaling 3611 s, were obtained on 2000 June 13 with the LWRS aperture centered on 12^h30^m49^s.1, +12°23'31" ($l = 283.77, b = +74.49$), about 7 arcsec from the galaxy's core. To reduce the data, we employ the CALFUSE pipeline (Sahnou et al. 2000; Oegerle, Murphy, & Kriss 2000), version 1.8.7, making two changes to the default parameters: first, we apply the pulse-height cut used for our cluster data, excluding photon events with pulse heights less than 4 or greater than 15 in standard arbitrary units; second, we rescale the assumed background count rate (which depends on the pulse-height

cut) until the residual continuum in the high- and medium-resolution apertures (which are essentially blank fields) is no more than 1–2% of the continuum in the LWRS aperture. To maximize the signal-to-noise ratio, the LiF 1A and LiF 2B spectra are shifted to a common wavelength scale (using the correction derived for Coma; see Dixon et al. 2001), weighted by their respective effective areas, averaged, and binned by 16 detector pixels. The resulting spectrum is presented in Fig. 1. The strongest absorption features are due to Galactic C II λ1036.34 and O I λ1039.23.

We generate a set of synthetic O VI absorption-line models using an ISM line-fitting package written at U.C. Berkeley by M. Hurwitz and V. Saba. Wavelengths, oscillator strengths, and other atomic data are taken from Morton (1991). Given the column density, Doppler broadening parameter, and a line list for each component, the program computes a Voigt profile for each absorption feature and outputs a high-resolution spectrum of τ versus wavelength. We adopt the Doppler parameter $b = 23$ km s⁻¹ appropriate for a 5×10^5 K gas. The model spectra are convolved with a Gaussian of FWHM = 80 km s⁻¹ (the observed width of the O I λ1039.23 feature) and rebinned to the resolution of our M87 spectrum.

Using SPECFIT, we fit our synthetic absorption profiles and a linear continuum to the 1030–1034 Å region of our M87 spectrum. The wavelength of the absorption feature is fixed at 1032.11 Å, the observed wavelength of the O VI λ1032 emission in the Virgo spectrum. The best-fit model (plotted in Fig. 1) corresponds to a column density $N(\text{O VI}) = (1.4 \pm 0.8) \times 10^{14}$ cm⁻², where the error bars represent $\Delta\chi^2 = 1$. The feature is statistically significant at the 2- σ level, but appears both weaker and narrower than the C II and O I lines. Our quoted column density may best be considered an upper limit.

Correcting the observed O VI doublet intensity $I_o \sim 5000$ photons cm⁻² s⁻¹ sr⁻¹ for scattering due to dust (a factor of about 1.5; see below) and self-absorption within the emitting cloud (a factor of about 2, though τ differs for the two components; see Shelton et al. 2001), yields an intrinsic O VI intensity toward Virgo of $I_i \sim 15,000$ photons cm⁻² s⁻¹ sr⁻¹. Using equation (5) of Shull & Slavin (1994), we combine I_i with $N(\text{O VI})$ towards M87 to derive the electron density n_e of the emitting plasma. Over the temperature range for which O VI is an important plasma constituent, $5.3 < \log T < 5.8$, n_e is nearly constant, varying between 0.046 and 0.048 cm⁻³ (though not monotoni-

cally), while the thermal pressure ($P_{\text{th}}/k = 1.92n_eT$) rises from 20,000 to 59,000 K cm⁻³. This calculation assumes that the O VI-emitting plasma has a constant emissivity per ion and that scattering by non-emitting species is negligible. If $N(\text{O VI})$ is considered an upper limit, then n_e and P_{th}/k are higher than the derived values.

5. DISCUSSION

Shelton et al. (2001) detect O VI emission at 1032 and 1038 Å with intensities of 2930 ± 290 and 1790 ± 260 photons cm⁻² s⁻¹ sr⁻¹, respectively, in an ~ 200 ksec *FUSE* observation centered on $l = 315.0, b = -41.3$. Though nearly antipodal, our sight lines show similar O VI intensities, suggesting that diffuse O VI emission with an observed doublet intensity of ~ 5000 photons cm⁻² s⁻¹ sr⁻¹ may be a general feature of high-Galactic-latitude sight lines.

Both the Coma and Virgo Clusters show up clearly in the *ROSAT* $\frac{1}{4}$ -keV surface-brightness map of Snowden et al. (1997). The plasma responsible for the observed soft-X-ray (SXR) flux is likely to be somewhat hotter than that producing our O VI emission. Also prominent in this map is the North Polar Spur (NPS), thought to be gas shock-heated to 10⁶ K by stellar winds and supernovae from hot stars in the Sco-Cen association (Weaver 1979; Heiles 1984). The Virgo Cluster lies near the edge of the SXR emission associated with the NPS.

The infrared emission maps of Schlegel, Finkbeiner, & Davis (1998) show that the Coma Cluster lies in a region of the sky nearly free of dust, with a reddening of only $E(B-V) = 0.008$. Assuming the extinction parameterization of Cardelli, Clayton, & Mathis (1989) and $R_V = 3.1$, this reddening corresponds to an attenuation of $\sim 10\%$ at 1035 Å. The infrared sky is more complex in the direction of the Virgo Cluster, as the cluster lies on the edge of a broad dust lane that may be associated with the NPS. The extinction toward Virgo is $E(B-V) = 0.030$. Any O VI $\lambda\lambda 1032, 1038$ emission originating beyond this obscuring material will be reduced in intensity by $\sim 34\%$ (hence our reddening correction of 1.5).

The column density $N(\text{O VI})$ derived from our M87 spectrum falls at the low end of the range $N(\text{O VI})$

$\sim (1.4 - 5.0) \times 10^{14}$ cm⁻² obtained by Savage et al. (2000) for sight lines through the Galactic halo. Such a low value of $N(\text{O VI})$ suggests that our Virgo sight line does not intercept significant O VI-emitting plasma associated with the North Polar Spur. If so, then parameters derived for this sight line may be typical of the Galactic halo. Given that the total pressure (thermal + nonthermal) in the Galactic plane may be as low as $\sim 25,000$ K cm⁻³ (McKee 1993), the thermal pressure we derive for the halo seems quite high. The derived thermal pressure would rise if $N(\text{O VI})$ is lower than our best-fit value, but would fall if the cirrus clouds responsible for dust extinction lie beyond the O VI-emitting plasma. Additional *FUSE* observations of M87, already scheduled for Cycle 2, should yield a greatly-improved determination of $N(\text{O VI})$.

As seen in Table 1, the LSR velocities of the O VI 1032 and 1038 Å emission features differ significantly from one another in both the Coma and Virgo spectra. Neither instrumental calibration uncertainties nor contamination by emission from other species can explain this effect. More likely, the apparent velocity differences are optical-depth effects. Because the optical depth of the 1038 Å line is half that of the 1032 Å line, the 1038 Å flux that we observe may have been emitted in regions far beyond those responsible for the 1032 Å flux. O VI component velocities from multiple sight lines may thus be used to map velocity fields in the Galactic halo, even when individual velocity components are not resolved.

Our serendipitous detection of diffuse O VI emission bodes well both for continued *FUSE* observations of selected sight lines and for proposed missions, such as *SPEAR* (*Spectroscopy of Plasma Evolution from Astrophysical Radiation*; Edelman, Korpela, & Dixon 2000), which seek to map the entire sky at FUV wavelengths.

We thank R. Shelton and E. Murphy for discussions of *FUSE* data analysis and acknowledge the outstanding efforts of the *FUSE* P.I. team to make this mission successful. This research has made use of NASA's Astrophysics Data System and is supported by NASA grant NAG 5-8956.

REFERENCES

- Avni, Y. 1976, *ApJ*, 210, 642
 Cardelli, J. A., Clayton, G. C., & Mathis, J. S. 1989, *ApJ*, 345, 245
 Dixon, W. V., Davidsen, A. F., & Ferguson, H. C. 1996, *ApJ*, 465, 288
 Dixon, W. V., Sallmen, S., Hurwitz, M., & Lieu, R. 2001, *ApJ*, 550, L25
 Ebeling, H., Edge, A. C., Bohringer, H., Allen, S. W., Crawford, C. S., Fabian, A. C., Voges, W., & Huchra, J. P. 1998, *MNRAS*, 301, 881
 Edelman, J., Korpela, E., & Dixon, W. V. 2000, *BAAS*, 32, 1427
 Heiles, C. 1984, *ApJS*, 55, 585
 Kriss, G. A. 1994, in *ASP Conf. Ser. 61, Astronomical Data Analysis Software and Systems III*, ed. D. R. Crabtree, R. J. Hanisch, & J. Barnes (San Francisco: ASP), 437
 Martin, C. & Bowyer, S. 1990, *ApJ*, 350, 242
 McKee, C. F. 1993, in *AIP Conf. Proc. 278: Back to the Galaxy*, ed. S. S. Holt & F. Verter (New York: AIP), 499-513
 Mihalas, D. & Binney, J. 1981, *Galactic Astronomy: Structure and Kinematics*, 2nd ed. (San Francisco: Freeman)
 Moos, H. W. et al. 2000, *ApJ*, 538, L1
 Morton, D. C. 1991, *ApJS*, 77, 119
 Oegerle, W., Murphy, E., & Kriss, G. 2000, *The FUSE Data Handbook* (<http://fuse.pha.jhu.edu/analysis/dhbook.html>)
 Sahnou, D. J. et al. 2000, *ApJ*, 538, L7
 Savage, B. D. et al. 2000, *ApJ*, 538, L27
 Schlegel, D. J., Finkbeiner, D. P., & Davis, M. 1998, *ApJ*, 500, 525
 Shelton, R. L. et al. 2001, *ApJ*, submitted
 Shull, J. M. & Slavin, J. D. 1994, *ApJ*, 427, 784
 Smith, R. J., Lucey, J. R., Hudson, M. J., Schlegel, D. J., & Davies, R. L. 2000, *MNRAS*, 313, 469
 Snowden, S. L. et al. 1997, *ApJ*, 485, 125
 Weaver, H. 1979, in *IAU Symp. 84: The Large-Scale Characteristics of the Galaxy*, ed. W. B. Burton (Dordrecht: Reidel), 295